# Fault impact analysis of ventilation systems in residential buildings

*A simulation-based case study in Denmark*

Marigo, Marco; Maccarini, Alessandro; Zarrella, Angelo; Afshari, Alireza

*Published in:*
Energy and Buildings

*DOI (link to publication from Publisher):*
10.1016/j.enbuild.2023.113150



*Publication date:*
2023

*Document Version*
Publisher's PDF, also known as Version of record

Energy & Buildings 292 (2023) 113150

Contents lists available at ScienceDirect

Energy & Buildings

journal homepage: www.elsevier.com/locate/enb

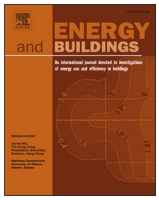

# Fault impact analysis of ventilation systems in residential buildings: A simulation-based case study in Denmark

Marco Marigo [a,*], Alessandro Maccarini [b], Angelo Zarrella [a], Alireza Afshari [b]

[a] Department of Industrial Engineering – Applied Physics Section, University of Padova, Via Venezia 1 – 35131, Italy
[b] Department of the Built Environment – Faculty of Engineering and Science, Aalborg University, A.C. Meyers Vænge 15, A, 6224 – 2450, København, Denmark

ARTICLE INFO

*Keywords:*
Fault impact analysis
Residential buildings
Ventilation
HVAC
Building simulation

ABSTRACT

The spread of intelligent buildings and advanced HVAC systems controls emphasizes the necessity of evaluating the impact of malfunctions caused by errors in the design, installation, or maintenance of these systems. In this work, the effect of the most diffused faults in ventilation systems is studied for an air handling unit installed in a Danish residential apartment. For this purpose, a dynamic model was built in Modelica, representing the building and the ventilation system. Different faults with varying intensities were implemented in the model. The impacts were evaluated by comparing the results of the obtained "with-fault" models with the "fault-free" model used as a benchmark. The comparison involved thermal and electrical energy use, thermal comfort and indoor air quality. Results showed that, for the studied system, the increase in thermal energy use was significant for the offset of the sensor controlling the bypass (up to + 27%), the bypass damper leakage and stuck (up to + 90%) and ducts' thermal losses (up to + 48%). In the latter case, an increase in thermal discomfort was observed (+7% of hours with operative temperature below 18.5 °C).

## 1. Introduction

### 1.1. Background

In recent years, research has been moving towards the new concept of "smart building" [1]. It is defined as "a residence that has been fitted out with technologies such as cloud computing that anticipates and responds to the needs of the occupants, working to improve their comfort, convenience, security, and entertainment by managing technology inside the residence and connecting them to other communities" [2]. This new approach deals with increasing involvement of technologies in buildings with continuous data collection, monitoring indoor environmental conditions and systems operations and carrying out actions aimed at actively controlling the indoor environment. The influence of this change in building management can be found in improving, among others, thermal comfort and indoor air quality. Another important aspect is using collected data for the building energy management system (BEMS). Its operations are addressed towards the energy efficiency issue, finding the configuration to optimize the use of HVAC systems to minimize energy use [3]. In these buildings, the high amount of available data allows the calculation of energy indicators that can be used to detect inefficiencies, taking actions aimed at improving real-time energy use [4].

The increasing necessity of managing energy use in buildings is related to the high consumption of the building sector that, according to European Commission data [5], is responsible for 40% of energy consumption and 36% of greenhouse gas emissions. In this context, the same European commission promotes innovation and investment in smarter buildings to contribute to energy efficiency.

The continuous search for efficient buildings with a more rational energy use can not ignore the difference between the design phase of construction and the operation, which sometimes causes energy waste due to defective installations or faulty system operations. Referring to variable air volume air handling units (VAV AHU), Torabi et al. listed the most impacting human-induced errors in the pre-, construction, and post-construction phases. They highlighted that most of them happen in the construction phase and are related to system control. They also recommend developing fault detection and diagnosis (FDD) methods and training programs for practitioners [6]. Another issue concerns failures occurring in systems independently of human action. The literature refers to these as faults, whose definition in IEA Annex 25 is "the departure from the normal operating point of a process" [7]. In this context, a new FDD-based approach has recently grown in importance; it

* Corresponding author.
*E-mail address:* marco.marigo@unipd.it (M. Marigo).

https://doi.org/10.1016/j.enbuild.2023.113150
Received 11 February 2023; Received in revised form 14 April 2023; Accepted 6 May 2023
Available online 8 May 2023

**Nomenclature**

*Shortcuts*

| | |
|---|---|
| *ACF* | After Crossflow Heat Exchanger |
| *AHC* | After Heating Coil |
| *AHU* | Air Handling Unit |
| *CAV* | Constant Air Volume |
| *CFHE* | Crossflow Heat Exchanger |
| *DCV* | Demand Controlled Ventilation |
| *EC* | Annual Electrical Use |
| *ECR* | Electrical Use Ratio |
| *EXT* | External |
| *FDD* | Fault Detection and Diagnosis |
| *FF* | Fault-Free |
| *FIA* | Fault Impact Analysis |
| *KPI* | Key Performance Indicator |
| *TE* | Annual Thermal Energy Use |
| *TER* | Thermal Energy Ratio |
| *TRY* | Test Reference Year |
| *VAV* | Variable Air Volume |

*List of symbols*

| | |
|---|---|
| $C$ | $CO_2$ concentration [ppm] |
| $C_L$ | Leakage class [(m L)/(s m$^2$)] |
| $Dp$ | Damper position [-] |
| $h$ | Heat transfer coefficient [W/(m$^2$ K)] |
| $Q_{leak}$ | Leakage rate [L/(s m$^2$)] |
| $T$ | Temperature [°C] |
| $\Delta p_s$ | Static pressure difference from duct interior to exterior [Pa] |
| $\varepsilon$ | Efficiency [-] |

*Subscripts*

| | |
|---|---|
| c | Convective |
| HC | Heating Coil |
| HS | Heating System |
| leak | Leakage |
| off | Offset |
| op | Operative |
| r | Radiant |
| tot | Total |
| WF | With-Fault |

was first applied to building HVAC systems in the '70 and became the focus of research from the '80 until nowadays [8]. In general, FDD is an area of investigation concerned with automating the processes of detecting faults with physical systems and diagnosing their causes [9], and its application to building systems is dealt with in the IEA annexes 25 and 34 [7,10]. Together with this approach, aimed at real-time detection of faults occurring in a system, the fault impact analysis (FIA) is a simulation-based approach whose aim is to study the fault influence on buildings' energy use, thermal comfort and indoor air quality (IAQ) [11]. For this purpose, a crucial point consists of the knowledge of the most impacting and frequent faults occurring in HVAC systems [7] and their modeling [11,12].

### 1.2. Literature review

The literature review highlighted the existence of various works where the simulation-based FIA was used as a methodology for the evaluation of improper systems operations and the quantification of impacts. This part will report the most relevant ones, focusing on the applied method, the obtained results, the used software and the analyzed case study.

Basarkar et al. present a detailed description of the implementation of a limited number of faults – clogging in a piping loop, economizer outdoor damper leakage, fouled heat exchanger and room sensor offset – in a simulation model of a large office building supplied by a variable air volume (VAV) system using EnergyPlus. Their presentation of the methodology applications is limited; however, they observed an increase in the total annual energy use of about 22% [13]. Almost the same approach was used by Andersen et al., which studied the presence of faults in a demand-controlled ventilation (DCV) system in an elementary school in Oslo (Norway). In this study, the increase in energy use is significant for some faults, reaching 77% and 60% in the case of supply and exhaust airflow sensor offset, respectively, but also impacts on thermal comfort and IAQ are analyzed [14]. Tallet et al. focus on a constant air volume (CAV) AHU installed in an office building. They studied the effect of sensor drift, valve leakage and duct leakage faults on energy consumption, thermal comfort and IAQ with Modelica with relevant results – an increase of energy use up to 2.75 times in summer and 1.25 times in winter – due to water valve leakage [15]. Yoon et al. also studied the single and combined effect of sensors' faults in HVAC systems in an office building with an AHU. They compared the annual energy use, machine performance (annual COP) and thermal comfort in different scenarios with different intensity sensor offsets. The authors observed that the temperature offsets at the building and air system levels had impacts on the overall system, particularly on energy performance and thermal comfort; the offsets in sensors at the water production system levels had local effects on the related system components [16]. The most comprehensive works in the FIA framework are those proposed in [17,18]. In the first case, the authors proposed a study on consumption and ventilation requirements in a DCV system installed in an office, analyzing different sensor offsets and comparing two methods, a probabilistic and a deterministic approach. In the deterministic analysis, with the evaluation of the single fault effect, the maximum deviation observed was a 17% energy use increase and an almost doubling number of under-ventilated hours (+94%). In the second study, they implemented 359 fault scenarios and performed weekly simulations with Modelica for a VAV system installed in an office building. Most of the faults resulted in having an impact lower than 6%; in some other cases, the effect was observed to be much higher, with different faults affecting the system's operation differently according to the season of operation.

Using white-box models for fault impact analysis is the first step for identifying the dominant effects with high detail and observing the impact of faults and their intensities on operating conditions. An evolution of this approach could be represented by the application of grey-box and inverse models, as suggested by Van Gelder et al. [19]. In this scenario, models could be incorporated into FDD tools and used to detect faults in real systems. An example of applying such a methodology is proposed by Gunay et al. [20].

### 1.3. Aim of the paper and novelty

The literature review highlighted that fault impact analysis is a widely used methodology for evaluating impacts due to faults in HVAC systems. However, except for a few works (e.g., [17,18]), the proposed analysis investigates a limited number of faults in narrow intensity ranges; in many cases, the investigation only concerns energy use and neglects the thermal comfort and IAQ aspects. Moreover, in the authors' knowledge, the application of FIA to a residential case study is missing in the literature.

The present paper aims to investigate the impacts due to the presence of faults in a CAV AHU installed in a typical Danish residential

apartment on thermal and electrical energy use, thermal comfort and indoor air quality. The building and the system models were created in Modelica, referred to in the literature as the most promising software for dynamic fault modeling [11]. A list of fault models was built, and the impact of each one, with different intensities, was studied through annual simulations.

## 2. Methodology

The proposed methodology is based on simulations with Modelica. In the first step, a fault-free model representing a typical Danish residential building was developed (*Section 2.1*). Consequently, specific faults for AHU systems were defined according to a literature review and added to the fault-free model, outlining the "with-fault model" (*Section 2.3*). In the subsequent step, KPIs were defined (*Section 2.4*) as the difference between fault-free and with-fault simulation results on relevant parameters. Finally, the KPIs were evaluated, showing how faults can affect energy use and indoor climate conditions.

### 2.1. Case study

#### 2.1.1. Building model

The building was modeled with the *AirMixed* model from the Modelica Buildings library [21]. It is a 98 $m^2$ residential apartment divided into two equal thermal zones: one with the living room and bedrooms, the other with the kitchen and bathroom. The two thermal zones are separated by a wall with an open door. In Fig. 1, the plan view of the building is shown. The south-oriented façade was exposed to the outdoor environment, whereas all the other surfaces were considered adiabatic.

This analysis studied three scenarios, each representing a different age in which buildings are modeled based on characteristic thermal performance. Table 1 shows the characteristics of each scenario.

For the windows reported in Table 1, the associated thermal transmittance is 5.4 W/($m^2$ K) for the single pane, 2.8 W/($m^2$ K) for the double pane and 2.0 W/($m^2$ K) for the triple pane window. The glass's thickness is 3 mm for all the typologies and a 12 mm air gap is considered for double and triple panes. The following boundary conditions were included in the model:

- Simulations were performed using climatic data from the TRY of Copenhagen [22].
- According to the Danish executive order on building regulations, constant air infiltration was set across the building envelope, equal to 0.09 L/(s m2), a reference value for residential buildings [23].
- Daily profiles for internal gains were assumed from European Standard EN 16798-1 [24]. The peak values correspond to 2.8 W/$m^2$ for people, 3 W/$m^2$ for appliances and 8 W/$m^2$ for lightning [25]; these values were split as 50% convective and 50% radiative. The latent heat gain was set at 1.4 W/$m^2$. All these values were given a time-dependent factor according to the schedules in the standard.

**Table 1**
Scenarios' thermal performance.

| Case Study | Opaque Wall Thermal Transmittance [W/($m^2$ K)] | Glazed Surfaces Typology [-] | Annual Energy Need [kWh/($m^2$ y)] |
|---|---|---|---|
| Scenario A | 0.6 | Triple pane | 25 |
| Scenario B | 1.1 | Double pane | 50 |
| Scenario C | 1.7 | Single pane | 100 |

#### 2.1.2. AHU and heating system models

The ventilation system analyzed in this study consists of a CAV AHU, whose layout represents a typical ventilation unit installed in a Danish residential building.

For this purpose, 29 ventilation system schematics were obtained by building managers in Denmark and analyzed. The most diffused layout chosen for the present work is represented in Fig. 2:

After filtering the incoming outdoor air, it undergoes heat recovery with exhaust air through a crossflow heat exchanger; after the rise in pressure given by the fan, air temperature is increased by the heating coil, whether it is not warm enough to be supplied to the room. The presence of a bypass system has a double purpose: during the cooling season, it allows the bypass of the heat recovery to provide external air at lower temperatures and fulfil thermal comfort requirements, whereas, in mid-seasons, it acts as a mixing valve between the air coming from outside and the heat recovery, guaranteeing the fulfilment of the set-point. According to Danish Standards, the considered system does not show the possibility of air recirculation as it should be avoided for health issues.

The system components were modeled using the followings settings:

- The supply and exhaust fans work at a constant mass flow rate equal to 0.3 L/(s $m^2$), the reference value for residential buildings according to Danish Standard [23].
- The crossflow heat exchanger works at a constant effectiveness of 0.8; the nominal pressure losses in each path were set at 200 Pa.
- The filters were modeled through the *FixedResistances.PressureDrop* model of the Modelica Buildings Library, which models the presence of the filter as a constant pressure drop; a nominal pressure drop of 40 Pa was assumed for each filter.
- In the fault-free model, ducts were modeled using the same method as filters, with a constant pressure drop of 150 Pa at nominal conditions.

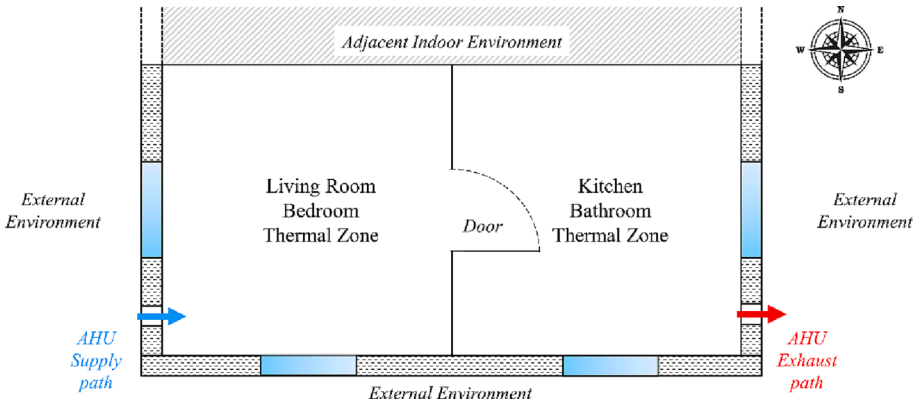


**Fig. 1.** Plan view of the residential apartment.

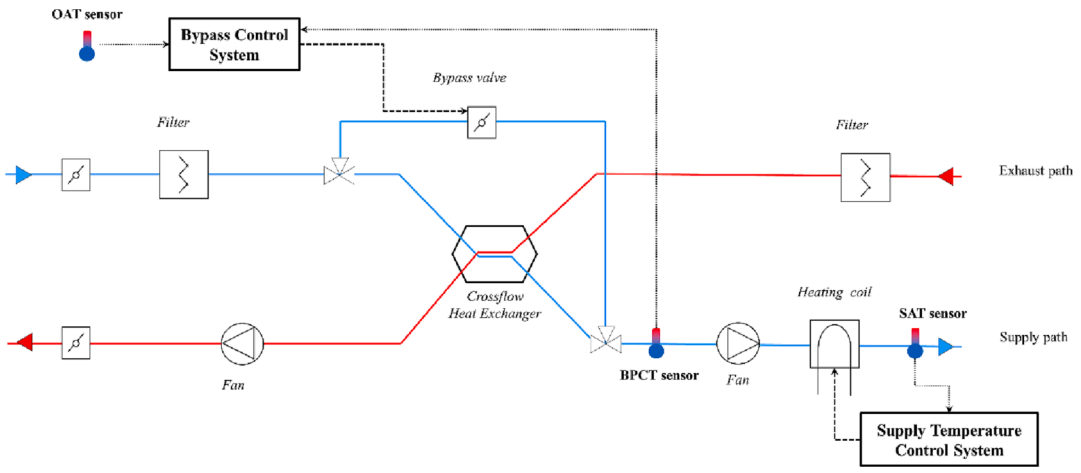


**Fig. 2.** Layout of the AHU.

- Before the air enters the crossflow heat exchanger, it is split into two parts through a junction; part of the airflow, whose amount is regulated by a damper, bypasses the heat recovery.
- The heating coil is modeled as a heat exchanger with constant effectiveness of 0.6; pressure losses were set at 50 Pa for the air side and 10 kPa for the waterside.
- A variable flow pump drives the hot water in the circuit, and the temperature increase is obtained through an ideal heater model (*HeatExchangers.Heater_T*) from the Modelica Buildings Library; the pump nominal flow rate was set to 0.0083 kg/s, whereas the boiler setpoint temperature was set to 40 °C. The total pressure losses in the water circuit were estimated at around 50 kPa.

The heating coil was dimensioned by assuming that the airflow temperature could be increased from the outdoor design temperature (-10 °C) to the supply temperature (18 °C). This resulted in a peak heating capacity of 970 W.

The control system mainly consists of two blocks controlling the pump's flow in the hot water circuit and the actuator of the bypass valve. In the first case, a PID controller was used to control the pump, which receives an input signal from the supply air temperature sensor placed after the heating coil. The supply air temperature was set to 18 °C. The PID was set for heating mode and switches on when the air needs an increase in temperature; otherwise, the heating coil is off. The bypass controller aims to reach 18 °C at the recovery unit outlet. The control logic of the bypass is shown in the diagram in Fig. 3.

In the case study analyzed in this work, the AHU only provides outdoor air to increase indoor air quality. In contrast, the building's heating is provided by an ideal system, whose sizing was made by calculating the peak of the annual heat load required for each case study for keeping the indoor temperature at 20 °C. The results for the three case studies showed a different sizing of the heating system, corresponding to 1.2 kW for Scenario A, 2.0 kW for Scenario B and 3.4 kW for Scenario C.

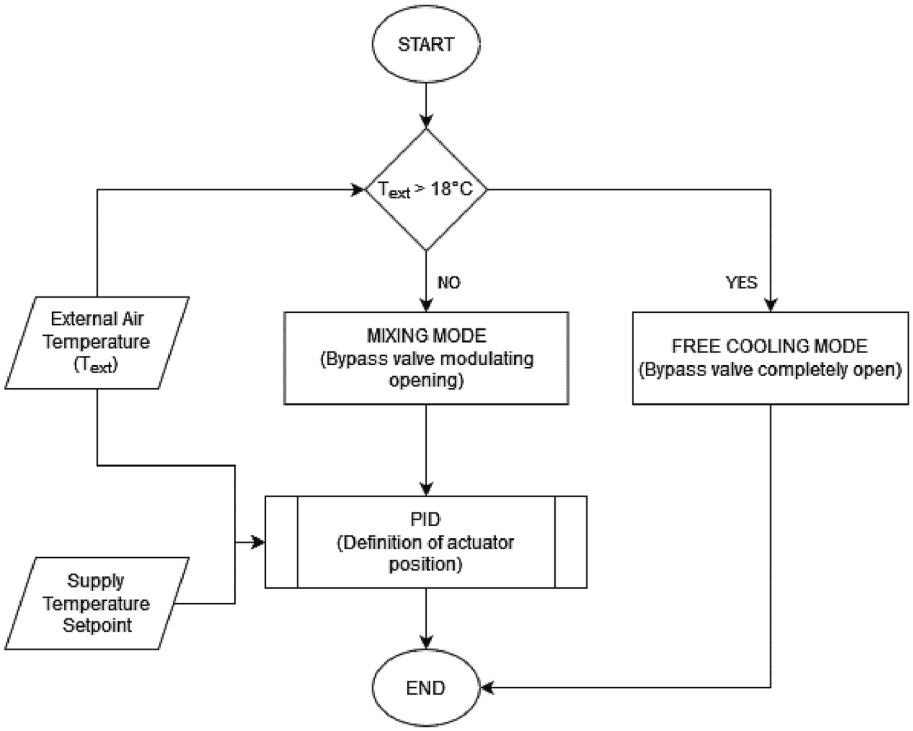


**Fig. 3.** Control system logic of the bypass valve.

### 2.2. Fault models

The literature review led to the definition of faults and related intensities frequently occurring in ventilation systems. Table 2 provides a summary of the faults implemented in this work.

Part of the fault models proposed was assumed from the existing papers highlighted in Table 2; some others were modeled considering their effect on the system's components. In this section, a full description of each fault is provided.

#### 2.2.1. Sensor offset model

The sensor offset model represents the incorrect reading of a sensor, which therefore detects a higher or lower value than the real one. In this work, its modeling is described by Eq. (1):

$$T_{WF} = T_{FF} + \Delta T_{off} \tag{1}$$

where $T_{WF}$ is the detected temperature by the faulty sensor, $T_{FF}$ is the same temperature in the fault-free case and $\Delta T_{off}$ is the offset intensity. A wrong calibration process or the reading degradation after a period without recalibration can cause the sensor offset. The presented model was applied to the ventilation system's sensors: the supply temperature sensor, whose measurement affects the operations of the heating coil, the temperature sensor at the heat recovery unit outlet and the external air sensors, controlling the bypass damper opening.

#### 2.2.2. Bypass damper leakage and stuck model

The faults associated with the bypass damper are stuck and the presence of air leakages. The stuck happens when the actuator is blocked in a particular position. The model of this fault is built by replacing the output of the bypass control system with a constant position signal ($Dp$). Different reasons can cause the damper to get stuck: it can be due to the control system not working properly or mechanical blocking of the actuator. Whether the valve tightness is not good enough, there can be air leakages across the bypass, with a portion of the airflow rate avoiding the heat recovery unit. The leakage model modifies the output of the bypass control system, establishing a minimum damper position, according to Eq. (2):

$$Dp_{WF} = \min(Dp_{FF},\ Dp_{leak}) \tag{2}$$

where $Dp_{WF}$ is the faulty damper position, $Dp_{FF}$ is the same parameter in the fault-free case and $Dp_{leak}$ is the minimum position associated with the presence of leakages.

**Table 2**
Fault list with intensity.

| Component | Fault | Intensity | References |
|---|---|---|---|
| Air temperature sensor at heating coil outlet | Sensor offset | [-4°C; +4°C] | [16,18,26–37] |
| Air temperature sensor at CFHE outlet | Sensor offset | [-4°C; +4°C] | |
| Outdoor air temperature sensor | Sensor offset | [-4°C; +4°C] | |
| Bypass Damper | Leakage | [0%,40%] | [18,28,33,36] |
| Bypass Damper | Stuck | [0%,100%] | [15,18,28,33,36] |
| Heating coil | Efficiency drop | [0.5; 0.6] | [13,18,27,32,38] |
| Crossflow heat exchanger | Efficiency drop | [0.7; 0.8] | |
| Air Filters | Fouling | Up to + 50% | [27,32] |
| Ducts | Leakage | $Q_{leak}$ = [0.14; 0.4] | [15] |
| Ducts | Poor insulation | 5 to 30 mm of insulation | [18] |
| Fan | Motor efficiency drop | Up to −30% | [18,33,34,39] |

#### 2.2.3. Crossflow heat exchanger degradation model

The efficiency drop of heat exchangers was modeled by substituting the nominal efficiency parameter of the crossflow heat exchanger with the parameter representing the fault. The main cause for efficiency drop is related to waterside scaling or air-side fouling of the heat exchanger. The efficiency values were therefore calculated assuming a range of thermal resistance increase from 5 to 50% due to fouling and scaling.

#### 2.2.4. Filter fouling model

Filter fouling is one of the most recurring faults in air systems, and it occurs in case of non-adequate maintenance and regular cleaning of filters. It was assumed that the filter resistance to the airflow could increase up to 50% because of fouling, reaching a value of 60 Pa compared to the 40 Pa adopted for clean filters. Similarly to other faults, the filter fouling is modeled by modifying the pressure drop due to the filter.

#### 2.2.5. Duct leakage and thermal losses model

The presence of leakages and thermal losses in ducts was also considered. In the first case, a leakage model was set up through the fixed resistance model of the Buildings library, which implemented in the simulations the leakage model proposed by ASHRAE in [40] based on Eq. (3):

$$Q_{leak} = C_L \Delta p_s^{0.65} \tag{3}$$

The calculation of the leakage flow rate ($Q_{leak}$) depends on the pressure difference between the inner and outer parts of the ducts ($\Delta p_s$), which is calculated at each timestep, and the leakage class ($C_L$), whose value is in [40]. The ducts' thermal losses were considered using the Pipe model of the Buildings library; it calculates the heat exchange between the fluid inside the ducts and the surrounding environment, assuming the insulation thickness and thermal conductivity as input.

### 2.3. Fault implementation and simulation settings

The faults presented in Section 2.2 were introduced once in the fault-free model, assuming constant intensity for the whole simulation time. By implementing each fault individually, 88 simulation cases were built, each consisting of a model with a specific fault and intensity.

The methodology choice involved the possibility of performing parametric simulations: each fault occurred alone in the system and its impact was evaluated individually with different simulations showing the effect of the increasing intensity.

Annual simulations with hourly timestep were performed with Modelica software [41].

### 2.4. KPIs

Each fault's impact was evaluated through Key Performance Indicators (KPIs), which define the gap between the fault-free and the with-fault case. In this work, the considered KPIs describe the impacts on energy use (electrical and thermal), thermal comfort and indoor air quality. In the next sections, a detailed description of KPIs is given for each class.

#### 2.4.1. Energy KPIs

The evaluations of the impacts of faults on energy use are presented in this work using four indexes: thermal energy use of the heating system, the thermal energy use of the AHU (e.g., thermal energy supplied to air by the heating coil), total thermal energy use, electrical energy use.

The KPIs are calculated considering the difference in the annual use between the faulty and the fault-free case, according to Eqs. 4–7:

$$TER_{HS} = \frac{TE_{HS,WF} - TE_{HS,FF}}{TE_{HS,FF}} \tag{4}$$

$$TER_{HC} = \frac{TE_{HC,WF} - TE_{HC,FF}}{TE_{HC,FF}} \quad (5)$$

$$TER_{tot} = \frac{(TE_{HS,WF} + TE_{HC,WF}) - (TE_{HS,FF} + TE_{HC,FF})}{(TE_{HS,FF} + TE_{HC,FF})} \quad (6)$$

$$ECR_{AHU} = \frac{EC_{AHU,WF} - EC_{AHU,FF}}{EC_{AHU,FF}} \quad (7)$$

In the above equations, the Thermal Energy Ratio (TER) and Electrical Consumption Ratio (ECR) are defined as the increase or decrease of consumption in each faulty case compared to the fault-free scenario in terms of annual Thermal Energy (TE) or Electrical Consumption (EC).

#### 2.4.2. Thermal comfort KPIs

Together with the energy impacts, the influence of faults on the thermal environment of the building was considered. The analysis was performed by comparing the hours when the operative temperature ($T_{op}$) lies within different predefined ranges (shown in Table 3) in the fault-free situation with each faulty condition. The operative temperature is defined as "the uniform temperature of an imaginary black enclosure in which an occupant would exchange the same amount of heat by radiation and convection as in the actual non-uniform environment" [42], and it is calculated according to Eq. (8):

$$T_{op} = \frac{h_c T_{air} + h_r T_r}{h_c + h_r} \quad (8)$$

The operating temperature ranges were established according to EN 16798-1 [22]. The fourth category in Table 3 is a representative range of category II of the standard; for higher operating temperatures (category 5), the indication of the standard is lower dissatisfaction of people, while categories 3, 2, 1 in Table 3 indicate a decreasing thermal comfort.

#### 2.4.3. Indoor air quality KPIs

The same approach used in Section 2.4.3 for thermal comfort analysis was also applied to the $CO_2$ concentration inside the building to evaluate the faults' impact on indoor air quality. The division in classes was taken from European Standard EN 16798 [24], and it is shown in Table 4:

## 3. Results and discussion

In the following sections, the results of the study are shown. The simulations' outputs are reported in *Section 3.1*. Subsequently, a discussion is offered about the coherence of the results and how each fault influences the system's behavior (*Section 3.2*).

### 3.1. Results

The obtained results are reported in this section following a four-step analysis. *Section 3.1.1* focuses on the ventilation system's total thermal energy and electrical consumption impacts. This analysis shows each fault's influence but neglects the variation of thermal energy produced by each system (e.g., heating system and heating coil). For this reason, in *Section 3.1.2*, the variation of each fault's intensity is analyzed in the two systems separately. The influence of different-age buildings is reported in *Section 3.1.3*, while the effects on thermal comfort and IAQ are shown in *Section 3.1.4*.

**Table 3**
Operative temperature ($T_{op}$) ranges proposed in this study.

| Categories | Operative Temperature |
|---|---|
| 1 | $T_{op} < 18.5$ °C |
| 2 | 18.5 °C $\leq T_{op} <$ 19.0 °C |
| 3 | 19.0 °C $\leq T_{op} <$ 19.5 °C |
| 4 | 19.5 °C $\leq T_{op} \leq$ 20.5 °C |
| 5 | $T_{op} >$ 20.5 °C |

**Table 4**
Ranges of the $CO_2$ concentration (C) for each IAQ class.

| Classes | $CO_2$ concentration ranges[1] |
|---|---|
| Class I | $C < 550$ ppm |
| Class II | 550 ppm $< C <$ 800 ppm |
| Class III | 800 ppm $< C <$ 1350 ppm |

[1] The indicated values are considered above outside.

#### 3.1.1. Impacts on thermal and electrical use

The first evaluation is performed considering the $TER_{tot}$ and $ECR_{AHU}$ indexes (see Section 2.4.1). The ratios refer to the energy use obtained from the fault-free simulation, 3106 kWh/y and 400 kWh/y for the total thermal and electrical consumption, respectively. The results are reported only for Scenario A; however, the considerations and conclusions made in this section are extendible to the other reported case studies. The effect of different building thermal performances is addressed in Section 3.1.3.

This analysis focuses on the total thermal energy and the ventilation system's electrical use. In the presented case study, these outputs highlight which faults can impact energy use and save the most. The analysis is based on final energy, neglecting the aspects of energy production systems that are beyond the scope of this paper.

In Fig. 4, the results of the fault sensors' impact are presented. The sensor after the heat recovery unit (ACF), which controls the air fraction bypassing the heat exchanger, strongly influences global thermal consumption. With a positive offset of 4 °C, the thermal energy consumption is almost 30% higher than the fault-free case. In the same scenario, a saving in electrical use can be observed due to the lower pressure losses of the bypass circuit. The temperature sensor after the heating coil (AHC) controls the hot water flow rate inside the heating coil. The most

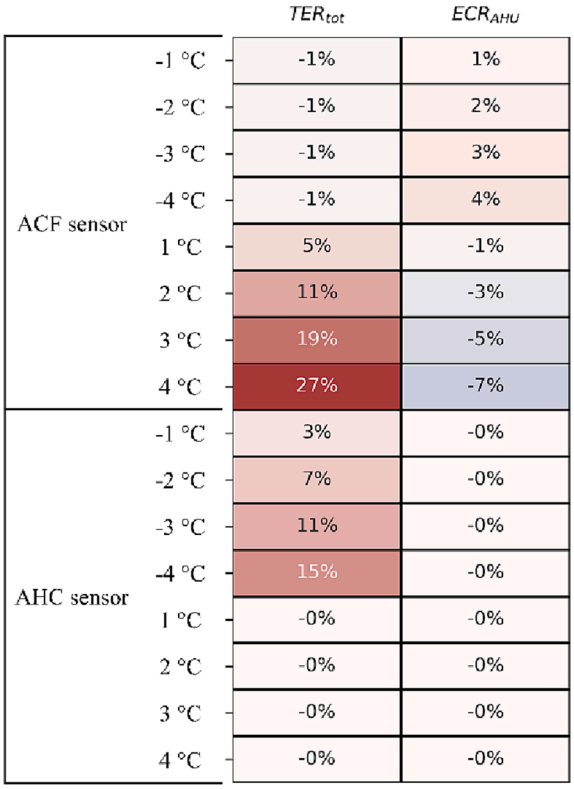


**Fig. 4.** Impact of ACF and AHC sensors offset with different intensities. The ratios are related to a fault-free scenario ($TE_{tot}$ = 3106 kWh/y, $EC_{AHU}$ = 400 kWh/y).

relevant impact can be found in the negative offset scenario, presenting a lower increase than the ACF sensor positive offset, but is still around 15% in the worst-case scenario. The external sensor offset is not given in this analysis, as it does not impact electrical or thermal energy use.

The poor operation of the bypass damper resulted in a high-impact fault (Fig. 5(a)). As presented in Section 2.2.2, leakage and stuck occur differently. However, in both cases, the fault intensity is referred to as the damper position (corresponding to the minimum reachable position for leakage and fixed position for stuck). Both thermal and electrical consumptions are affected by bypass fault, as it acts on the share of airflow passing through the crossflow heat exchanger, modifying the air path pressure losses and the heat recovered. The leakage fault can increase thermal energy consumption by 30% (with 7% electrical savings), but the stuck impact is higher. The two border scenarios are $Dp_F = 0$ and $Dp_F = 1$, which outline the cases with fully closed (maximum heat recovered) and fully open (zero heat recovered) bypass damper positions, respectively. The fully closed case has no relevant impact (except for a 7% increase in electricity consumption); instead, the fully open damper almost doubles the thermal energy consumption.

The duct faults (Fig. 5(b)) outline a different relevance between the duct leakage and the thermal loss faults. The latter strongly influences the total thermal consumption, up to about 50% in the case of a 5 mm thickness of duct insulation. In contrast, only the electrical consumption seems slightly affected by duct leakage. This aspect is justified by the low leakage flow obtained following ASHRAE's leakage model: in the worst-case scenario ($C_L = 0.4$), the leakage flowrate ranges, according to pressure variations, between 0.0007 and 0.0016 kg/s, 2% and 4.6% of the nominal flow rate, respectively.

The efficiency drop of the heat recovery unit was observed to have an impact that can reach almost the 10% in the total thermal consumption, with a maximum difference in efficiency equal to 0.1 (compared to the 0.8 value for the fault-free scenario) (Fig. 6).

In Fig. 7, the faults affecting only the electricity consumption are reported. In both cases, only the supply duct was considered in the single component fault; however, the fouled return filter or return fan efficiency drop showed the same results as the supply. Results show a greater impact of motor degradation (up to 40% with both components' fault) than filter fouling (up to 5%).

### 3.1.2. Impacts of fault intensity on systems behaviour

This section aims to provide a view of how different faults and intensities impact single thermal energy systems' consumption. The results are shown according to the $TER_{HS}$ and $TER_{HC}$ indexes, referring to the consumption of the fault-free case.

As described in Section 2.1.2, it was decided to limit the power of the heating system and heating coil to provide more realistic operations. It should be noted that the choice of the systems' peak power and their interaction (e.g., the control system) affect the results shown in this part.

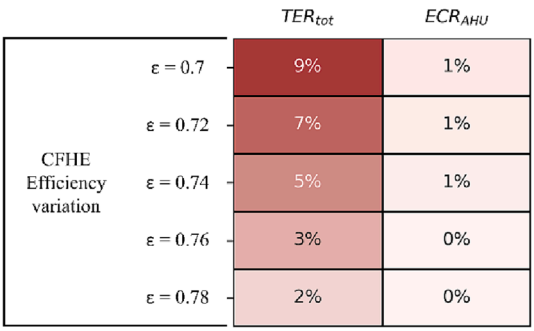


**Fig. 6.** Impact of performance degradation of the crossflow heat exchanger. The ratios are related to a fault-free scenario ($TE_{tot}$ = 3106 kWh/y, $EC_{AHU}$ = 400 kWh/y).

Besides the EXT sensor offset, whose influence is restrained in the proposed case study, Fig. 8 shows how energy is shared between the two systems. The ACF sensor's negative offset decreases heating system consumption (up to −1.5%), whereas the positive offset increases the energy exchanged by the heating coil (up to + 400%). These effects cause a decrease in the negative offset and an increase in the positive offset scenarios of the total energy consumption, as discussed in Fig. 4. Conversely, in the case of the AHC sensor, the positive offset does not show a growth of the total thermal consumption: the decrease in energy supplied by the heating coil (in the case of + 4 °C offset the heating coil is off for the whole year) is compensated by an increase in the heating system's consumption. In the negative offset scenario, the increase in the heating coil consumption (up to 560%) does not correspond to the decrease in heating system thermal energy (around −25%), taking to the increase in total energy already discussed in the previous section.

Analyzing the bypass faults (Fig. 9), almost the whole energy consumption increase is associated with the increased heating coil operation, which reports increased consumption by up to + 450% for the leakage and + 1340% for the stuck. In the case of a fully closed damper position scenario ($Dp_F = 0$), "forcing" the supply air into the heat recovery unit for the whole year involves some savings in the heating consumption, although limited (-1.5%).

The inadequate duct insulation affects both systems (Fig. 10), with an increase of 25% for the heating system and 380% for the heating coil consumption in the 5 mm insulation thickness scenario. Unlike other faults, the thermal losses are not concentrated in a part of the system, but air undergoes continuous transformation along with the duct length. For this reason, despite their dependence on the adjacent environment and duct paths, thermal losses are potentially one of the faults that have a greater effect on consumption and system operation.

The effect on leakage, almost irrelevant in the total thermal consumption, show an increase in the heating coil consumption due to the

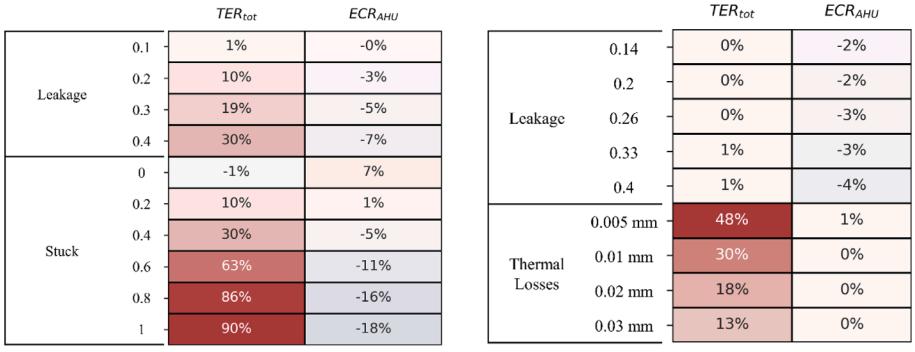


**Fig. 5.** Impact of bypass damper leakage and stuck fault (a) and ducts' leakage and thermal losses (b). The ratios are related to a fault-free scenario ($TE_{tot}$ = 3106 kWh/y, $EC_{AHU}$ = 400 kWh/y).

| | | $TER_{tot}$ | $ECR_{AHU}$ |
|---|---|---|---|
| Both Fans | $\eta_{el} = 0.5$ | 0% | 40% |
| | $\eta_{el} = 0.55$ | -0% | 27% |
| | $\eta_{el} = 0.6$ | -0% | 17% |
| | $\eta_{el} = 0.65$ | -0% | 8% |
| Supply Fan | $\eta_{el} = 0.5$ | -0% | 20% |
| | $\eta_{el} = 0.55$ | -0% | 14% |
| | $\eta_{el} = 0.6$ | -0% | 8% |
| | $\eta_{el} = 0.65$ | -0% | 4% |

*(a)*

| | | $TER_{tot}$ | $ECR_{AHU}$ |
|---|---|---|---|
| Both Filters | $\Delta P = 45$ Pa | 0% | 1% |
| | $\Delta P = 50$ Pa | -0% | 3% |
| | $\Delta P = 55$ Pa | -0% | 4% |
| | $\Delta P = 60$ Pa | -0% | 5% |
| Supply Filter | $\Delta P = 45$ Pa | -0% | 1% |
| | $\Delta P = 50$ Pa | -0% | 1% |
| | $\Delta P = 55$ Pa | -0% | 2% |
| | $\Delta P = 60$ Pa | -0% | 3% |

*(b)*

**Fig. 7.** Impact of fans' electrical efficiency drop (a) and filter fouling (b). The ratios are related to a fault-free scenario ($TE_{tot}$ = 3106 kWh/y, $EC_{AHU}$ = 400 kWh/y).

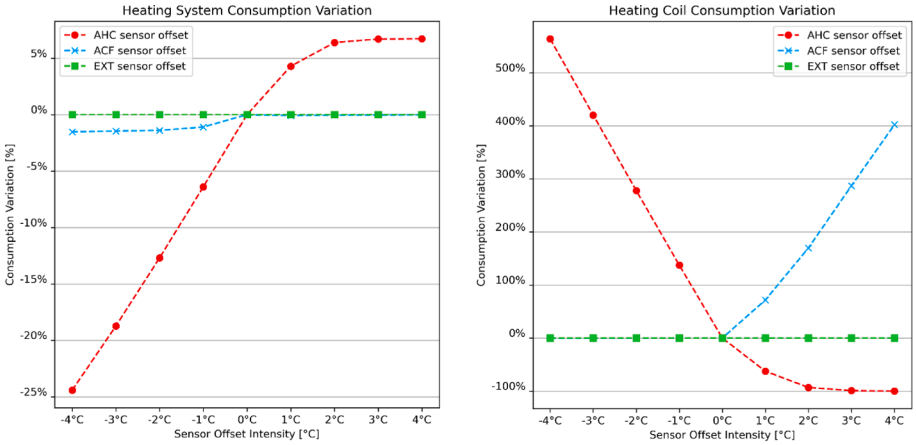


*(a)* *(b)*

**Fig. 8.** Impact of sensor offset intensity on heating system (a) and heating coil (b) consumptions. The ratios are related to a fault-free scenario ($TE_{HS}$ = 2898 kWh/y, $TE_{HC}$ = 208 kWh/y).

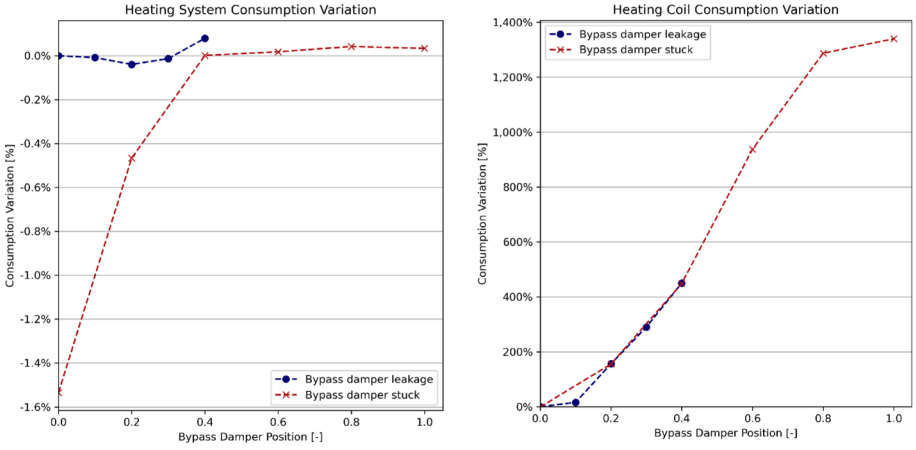


*(a)* *(b)*

**Fig. 9.** Impact of bypass damper faults intensity on heating system (a) and heating coil (b) consumptions. The ratios are related to a fault-free scenario ($TE_{HS}$ = 2898 kWh/y, $TE_{HC}$ = 208 kWh/y).

lower temperature of the leaking air inside the ducts (Fig. 11). However, the most relevant aspect is the decreased supply flow rate, involving a lower IAQ; this aspect will be discussed in the following paragraphs.

### 3.1.3. *Impacts on different-age buildings*

The variation of impact with building age and the envelope's thermal performance is analyzed in this section, and the results are shown in Table 5. It was decided to display the most impactful faults with the higher intensity to have an overview of the building age effect.

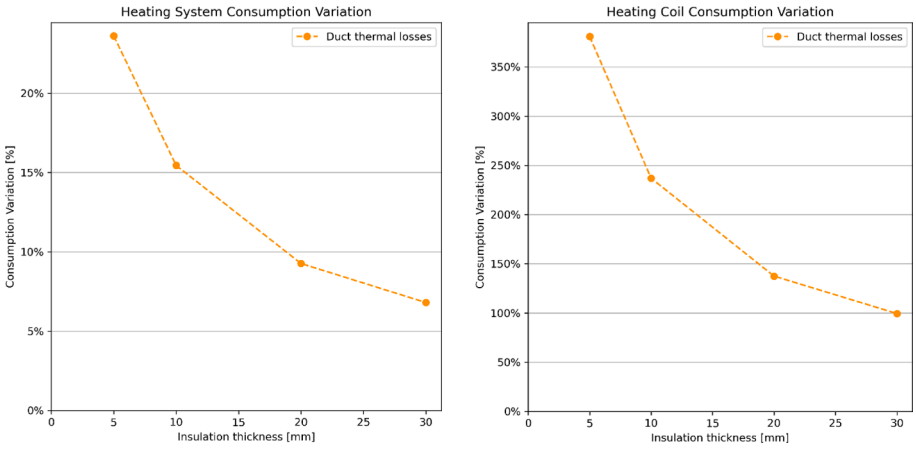


(a) (b)

**Fig. 10.** Impact of duct insulation thickness on heating system (a) and heating coil (b) consumptions. The ratios are related to a fault-free scenario ($TE_{HS}$ = 2898 kWh/y, $TE_{HC}$ = 208 kWh/y).

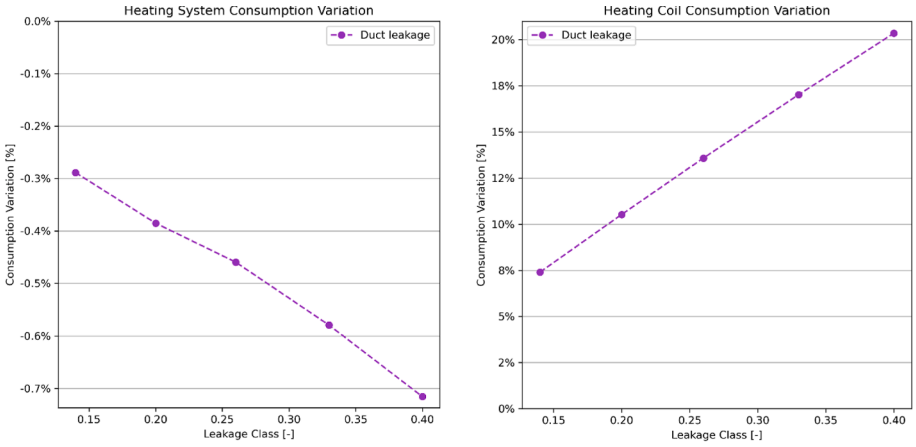


(a) (b)

**Fig. 11.** Impact of duct leakage flow rates on heating system (a) and heating coil (b) consumptions. The ratios are related to a fault-free scenario ($TE_{HS}$ = 2898 kWh/y, $TE_{HC}$ = 208 kWh/y).

**Table 5**
Impact of faults in buildings with different insulation levels. The Energy Ratio is referred to the fault-free total thermal consumption: 3106 kWh/y for the recent, 5597 kWh/y for the medium and 10,403 kWh/y for the old building.

| Component | Fault | Intensity | $TER_{tot}$ Scenario A | Scenario B | Scenario C |
|---|---|---|---|---|---|
| ACF sensor | Offset | +4 °C | 27% | 15% | 8% |
| AHC sensor | Offset | −4 °C | 13% | 7% | 3% |
| Bypass valve | Valve stuck | Fully-open | 90% | 50% | 27% |
| Bypass valve | Valve leakage | $Dp$ = 0.4 | 30% | 17% | 10% |
| Ducts | Thermal losses | Insulation = 5 mm | 48% | 27% | 14% |
| CFHE | Efficiency drop | $\varepsilon$ = 0.7 | 9% | 5% | 3% |

The reported results show that the impact of each fault is higher in buildings with higher thermal performance in terms of the total thermal energy ratio. The calculation of the consumption difference between the simulation with and without faults gives similar results in the different-age case studies: the faults affect the ventilation system operations, which are independent of indoor environmental conditions. However, the higher percentage of thermal energy ratio in recent buildings proves that the better the building's thermal performance, the more significant the impact of the HVAC system fault becomes.

### 3.1.4. *Impacts on thermal comfort and IAQ*

In some of the simulated cases, it was observed that the presence of a fault could affect the thermal comfort or IAQ aspects. The first case happens when the faults are such severe that, due to the limit imposed on the heating system and heating coil, the systems are not able to fulfill the energy requirements of the building. This scenario results in unmet thermal comfort hours.

In the case of the AHC sensor fault (Fig. 12), a general decrease in thermal comfort can be observed with a positive offset. In the + 4 °C intensity value, the hours when the $T_{op}$ is below 18.5 °C drop from 0.2% (FF case) to 1.4%; similarly, considering the operative temperature range between 18.5 and 19.0 °C, the share varies from 1.6% to 2.6%. The negative offset scenario presents a higher average $T_{op}$, e.g., hours in the warmer temperature range change from 46.3% to 48.7%. Improved comfort conditions, however, must be contextualized within a scenario of growing consumption, as highlighted in Section 3.1.1.

Compared to AHC sensor offset, more significant degradation of indoor thermal comfort is found for low insulation ducts, as shown in Fig. 13. In the lower classes for thermal comfort, $T_{op}$ < 18.5 °C and

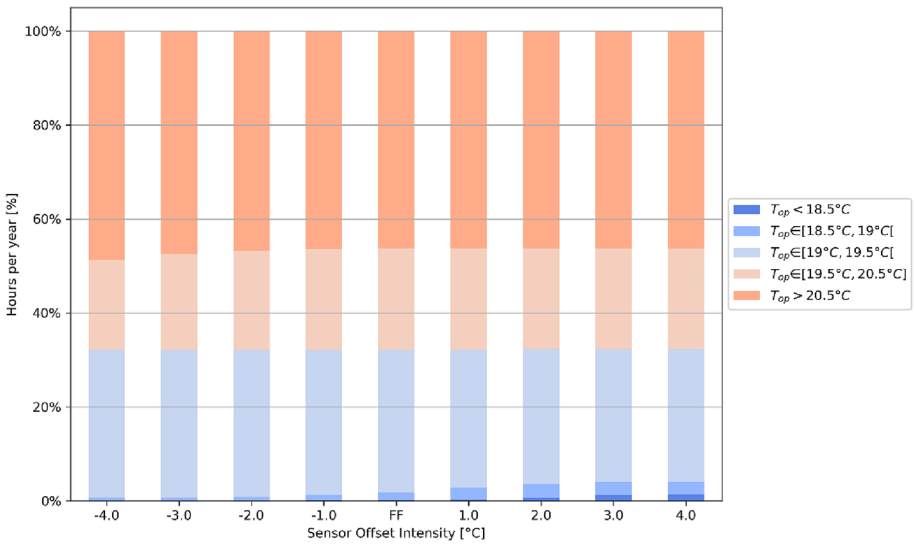


**Fig. 12.** Variation of the hours in each operative temperature range in different AHC sensor offset scenarios.

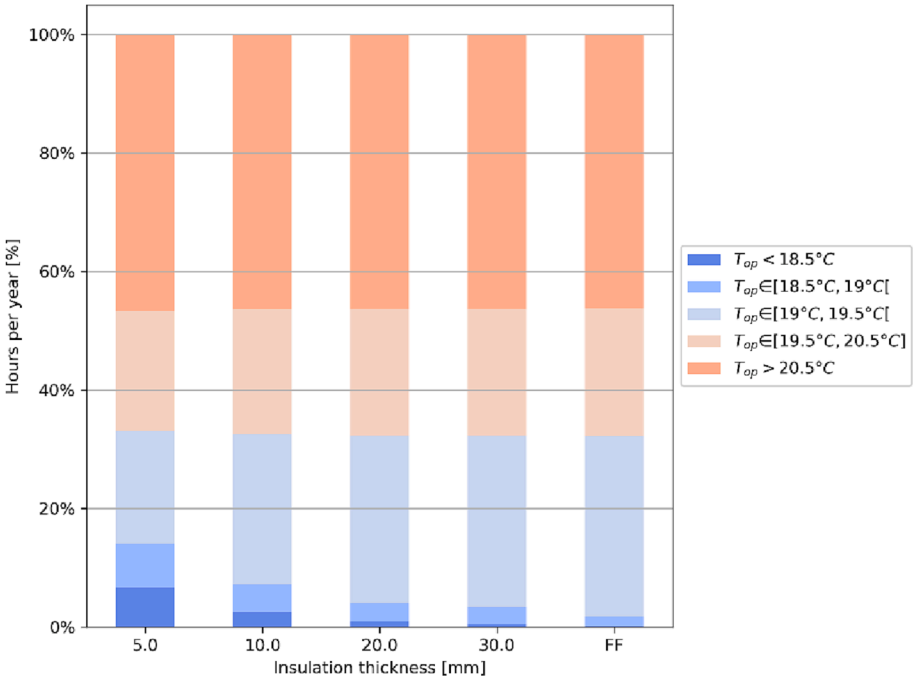


**Fig. 13.** Variation of the hours in each operative temperature range in different insulation thickness scenarios.

18.5 °C ≤ $T_{op}$ < 19.0 °C, the share changes from the 0.2% and 1.6% of the FF case study to the 6.6% and 7.3% of the ducts' thermal losses scenario.

On the other side, it was observed that, despite not having important impacts on thermal and electrical energy consumption, leakage in the ducts decreases the air supplied to the building, causing lower IAQ in the indoor environment (Fig. 14). The simulation of the FF scenario shows that 83% of the time, the ventilation system can guarantee good air quality, reaching Class I according to the European Standard [24]. In the worst-case scenario, with a leakage rate of 0.4, the share is lowered to 75% of the annual time; while 25% of the time, Class II is detected, where the CO2 concentration is above 550 ppm.

### 3.2. Faults' effect on the system's behavior

Faults in HVAC systems affect each sub-component's plant behavior and operations. In the following sections, the discussion of the results is reported to investigate this aspect.

#### 3.2.1. Sensors offset

The AHC sensor detects the air temperature at the heating coil outlet and controls the water flow rate to reach the air supply temperature setpoint (18 °C). The positive offset causes a higher detected air temperature than the real one, leading to a decrease in the water flow rate and, consequently, a lower temperature of the air supplied by the ventilation system. The reduction of the thermal energy consumption of the heating coil with an increasing positive offset (Fig. 8(b)) would result in a lower indoor air temperature, but this is balanced by an increase in heating system consumption (Fig. 8(a)). Therefore, the AHC sensor positive offset does not increase the total energy consumption (Fig. 4) but involves a different balance between the two systems. The negative offset acts in reverse, increasing the water flow rate and the

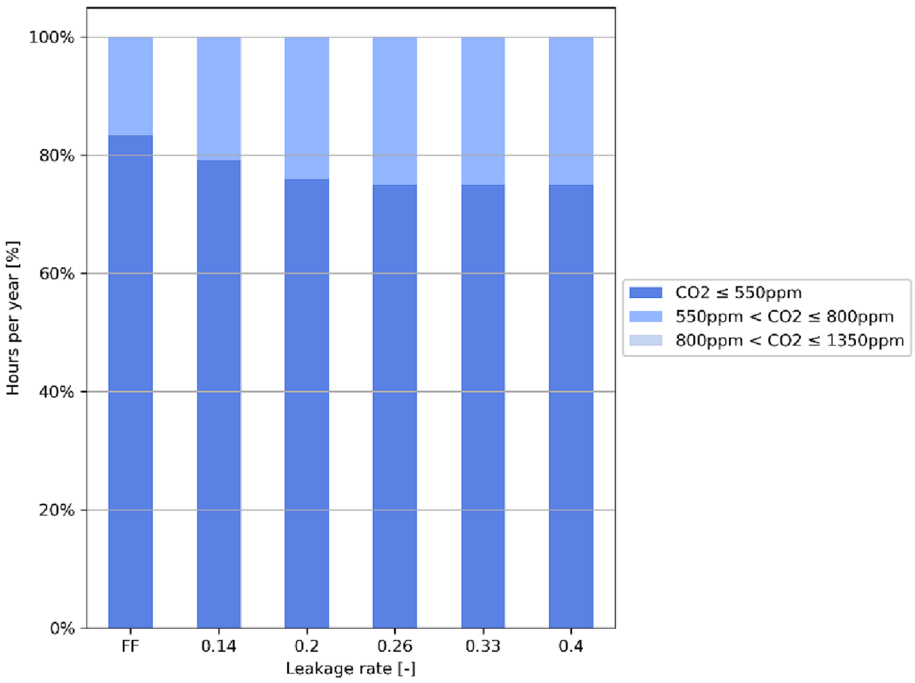


**Fig. 14.** Hours' variation for each IAQ class based on $CO_2$ concentration above outside in different duct leakage scenarios.

thermal consumption of the heating coil (Fig. 8(b)). The heating system decreases consumption (Fig. 8(a)); however, an increase in the total thermal consumption can be observed (Fig. 4), involving a higher temperature inside the building with the risk of overheating (Fig. 12).

The ACF sensor detects the air temperature after mixing the bypass and the heat recovery path and controls the bypass flow to reach the setpoint temperature value (18 °C). When a positive offset occurs, the detected temperature is higher than the real one, and the control system opens the bypass damper more than needed. The consequence is a lower heat recovered, whose missing amount is supplied by the heating coil, which shows an increase in consumption (Fig. 8(b)). The air supply temperature does not change; hence a decrease in heating system consumption does not occur (Fig. 8(a)), increasing the total thermal consumption (Fig. 4). The negative offset involves a longer time for the bypass damper to stay closed and a lower opening level. Higher supply air and indoor temperature (in some time ranges) are found, but this occurs when the heating coil remains off. Therefore, the savings in total energy consumption are limited (Fig. 4). The changes in electrical consumption are due to the different airflow rates crossing the heat recovery unit, which causes higher pressure losses. For this reason, the electrical consumption decreases when the amount of air in the bypass path increases (positive offset) and increases in the opposite situation (negative offset) (Fig. 4).

In this work, the external temperature sensor behavior does not affect the system's operation: it forces the full opening of the bypass damper when outdoor conditions are favorable ($T_{ext} > 18$ °C), which generally already occurs with the control provided by ACF sensor, dealing in neglecting impacts with the positive or negative offset of EXT sensor (Figs. 4, 8).

### 3.2.2. *Bypass faults*

The leakage fault occurs when an undesired airflow ratio bypasses the crossflow heat exchanger due to unsealed damper closing. The electrical consumption decreases for a lower flow in the heat recovery unit with increased leakage, but this involves a lower heat recovered and an increasing need for integration provided by the heating coil, which is reflected in an increase in total heat consumption of up to 30%, although heating system consumption remains unchanged (Fig. 5(a), 9).

The stuck fault differs from leakage as it corresponds to a situation with a fixed damper position for the whole simulation time. Despite this difference, the results are similar to those presented for leakage fault: the thermal energy consumption increases as the stuck occurs at a higher opening level because the heat recovery decreases. The heating coil provides the whole amount of energy to reach the supply air temperature setpoint (Fig. 9). An opposite trend is shown by the electrical consumption, which decreases with the opening of the bypass valve for the lower pressure losses in the bypass path (Fig. 5(a)).

### 3.2.3. *Ducts faults*

The ducts' leakage fault does not greatly impact total thermal consumption. However, it is shown in Fig. 11 that the heating coil increases the consumption due to the inlet leakage of air colder than that coming from the heat recovery process. With the analyzed leakage rate, the heating coil can provide the energy needed to keep the supply air setpoint temperature. This fault involves a lower airflow inside the ducts and supplied to the room, which is the cause for the lower heating system consumption (Fig. 11(a)): it is referred to the energy the system should use to take the missing air from the supply (18 °C) to the indoor (20 °C) temperature setpoint. The impact of a lower flow is also reflected in the electrical consumption, which is lower than the simulation without leakages (Fig. 5(b)), but it also entails a lower IAQ level inside the building, as shown in Fig. 14.

As discussed in Section 3.1.2, the ducts' thermal losses affect all the air paths and components operations. The heating coil consumption increases because of the lower air temperature entering the crossflow heat exchanger caused by exhaust duct losses and the losses in the supply path before the heat integration (Fig. 11(b)). However, the supply temperature setpoint is not reached in this case for the thermal losses in the duct's track after the heating coil; an increase in thermal consumption of the heating system is therefore observed (Fig. 11(a)). For the high amount of losses, in the most critical hours of the year, the systems can not provide the whole thermal energy needed to keep the indoor temperature setpoint, an increase of unmet hours for thermal comfort is found (Fig. 13).

## 4. Conclusion

The present study investigated the presence of faults in a ventilation system composed of a constant air volume (CAV) air handling unit (AHU) installed in a Danish residential apartment. Annual simulations were performed with Modelica to study the effect of single faults by comparing the output (energy use, operative temperature, indoor $CO_2$ concentration) of a "fault-free" baseline model and "with-fault" models. For the present case study, the following results were obtained:

- Poor bypass damper operations are the main causes of increased thermal energy use, which can result in almost double the baseline scenario (+90%, in case of fully open stuck). Ducts' poor insulation and sensors offset (especially AHC and ACF sensors) are also impactful for thermal energy use.
- Fans' efficiency drop of up to 10% can lead to a relevant increase in electrical energy use (up to + 40%).
- Most of the analyzed faults cause imbalanced operations between the systems in the building (e.g., ventilation and heating systems). When the plant cannot compensate for these unbalances, thermal discomfort and low-IAQ hours occur (duct leakage and thermal losses faults, AHC sensor offset).
- The effect of the fault presence is higher in buildings with higher thermal performance; therefore, more attention in the design and maintenance phase is required in these cases.

The results obtained are useful for producers of these systems, helping the design process and giving awareness of the impact that poor operations (installation, improper design, inadequate maintenance) can have on a system's energy use. However, the results obtained are strictly correlated to the choice of boundary conditions; this leads to the necessity of a wider application of this methodology to investigate the effects of faults in different operative conditions. A more complex scenario deals with the coexistence of more simultaneous faults, which has not been studied in the present paper and could be an interesting further application of this methodology.

The white-box modeling approach proposed in this work can be considered a first step to studying the faults' effect on the system in depth. Starting from these results, a scalability approach can be developed considering inverse modeling for a detailed system; in this case, grey-box or black box models can be interesting solutions that could be implemented in FDD tools for more efficient detection of faults.

## Declaration of Competing Interest

The authors declare that they have no known competing financial interests or personal relationships that could have appeared to influence the work reported in this paper.

## Data availability

Data will be made available on request.

## Acknowledgment

This study was financially supported by the National Building Fund (Landsbyggefonden).

## References

[1] A.H. GhaffarianHoseini, N.D. Dahlan, U. Berardi, A. GhaffarianHoseini, N. Makaremi, The essence of future smart houses: From embedding ICT to adapting to sustainability principles, Renew. Sustain. Energy Rev. 24 (2013) 593–607, https://doi.org/10.1016/j.rser.2013.02.032.
[2] M. AlMuharraqi, G. Sweis, R. Sweis, F. Sammour, Factors affecting the adoption of smart building projects in the Kingdom of Bahrain, J. Build. Eng. 62 (2022), 105325, https://doi.org/10.1016/j.jobe.2022.105325.
[3] P. Rocha, A. Siddiqui, M. Stadler, Improving energy efficiency via smart building energy management systems: A comparison with policy measures, Energy Build. 88 (2015) 203–213, https://doi.org/10.1016/j.enbuild.2014.11.077.
[4] M. Peña, F. Biscarri, J.I. Guerrero, I. Monedero, C. León, Rule-based system to detect energy efficiency anomalies in smart buildings, a data mining approach, Expert Syst. Appl. 56 (2016) 242–255, https://doi.org/10.1016/j.eswa.2016.03.002.
[5] European Commission, Energy efficiency in buildings, (2020). https://commission.europa.eu/news/focus-energy-efficiency-buildings-2020-02-17_en (Accessed February 8th, 2023).
[6] N. Torabi, H.B. Gunay, W. O'Brien, T. Barton, Common human errors in design, installation, and operation of VAV AHU control systems – A review and a practitioner interview, Build. Environ. 221 (2022), 109333, https://doi.org/10.1016/j.buildenv.2022.109333.
[7] M.W. Liddament, Real Time Simulation of HVAC Systems for Building Optimisation, Fault Detection and Diagnostics - Technical Synthesis Report IEA Annex 25, 1999. http://www.iea-ebc.org/fileadmin/user_upload/docs/EBC_Annex_25_tsr.pdf.
[8] B. Yu, D.H.C. Van Paassen, S. Riahy, General modeling for model-based FDD on building HVAC system, Simul. Pract. Theory 9 (2002) 387–397, https://doi.org/10.1016/S1569-190X(02)00062-X.
[9] S. Katipamula, M.R. Brambley, Review article: Methods for fault detection, diagnostics, and prognostics for building systems—A review, part I, HVAC R Res. 11 (2005) 3–25, https://doi.org/10.1080/10789669.2005.10391123.
[10] R. Jagpal, Technical Synthesis Report IEA Annex 34: Computer Aided Evaluation of HVAC System Performance, 2006. https://www.iea-ebc.org/Data/publications/EBC_Annex_34_tsr.pdf (Accessed February 8th, 2023).
[11] Y. Li, Z. O'Neill, A critical review of fault modeling of HVAC systems in buildings, Build. Simul. 11 (2018) 953–975, https://doi.org/10.1007/s12273-018-0458-4.
[12] P. Haves, Fault modelling in component-based HVAC simulation, Proc. Build. Simulation'97. (1997).
[13] M. Basarkar, X. Pang, L. Wang, P. Haves, T. Hong, Modeling and simulation of HVAC faults in EnergyPlus, Proc. Build. Simul. 2011 12th Conf. Int. Build. Perform. Simul. Assoc. (2011) 2897–2903.
[14] K. Heimar Andersen, S.B. Holøs, A. Yang, K. Thunshelle, Ø. Fjellheim, R. Lund Jensen, Impact of Typical Faults Occurring in Demand-controlled Ventilation on Energy and Indoor Environment in a Nordic Climate, E3S Web Conf. 172 (2020) 1–8, https://doi.org/10.1051/e3sconf/202017209006.
[15] A. Tallet, M.M.K. Merghani, C. Inard, Air Handling Unit Faults Impact on Thermal Comfort, Energy Consumption and Indoor Air Quality in an Office Building, in: CLIMA2016, 2016.
[16] S. Yoon, Y. Yu, J. Wang, P. Wang, Impacts of HVACR temperature sensor offsets on building energy performance and occupant thermal comfort, Build. Simul. 12 (2019) 259–271, https://doi.org/10.1007/s12273-018-0475-3.
[17] X. Lu, Z. O'Neill, Y. Li, F. Niu, A novel simulation-based framework for sensor error impact analysis in smart building systems: A case study for a demand-controlled ventilation system, Appl. Energy. 263 (2020), 114638, https://doi.org/10.1016/j.apenergy.2020.114638.
[18] X. Lu, Y. Fu, Z. O'Neill, J. Wen, A holistic fault impact analysis of the high-performance sequences of operation for HVAC systems: Modelica-based case study in a medium-office building, Energy Build. 252 (2021), 111448, https://doi.org/10.1016/j.enbuild.2021.111448.
[19] L. Van Gelder, P. Das, H. Janssen, S. Roels, Comparative study of metamodelling techniques in building energy simulation: Guidelines for practitioners, Simul. Model. Pract. Theory. 49 (2014) 245–257, https://doi.org/10.1016/j.simpat.2014.10.004.
[20] B. Gunay, B.W. Hobson, D. Darwazeh, J. Bursill, Estimating energy savings from HVAC controls fault correction through inverse greybox model-based virtual metering, Energy Build. 282 (2023), 112806, https://doi.org/10.1016/j.enbuild.2023.112806.
[21] Lawrence Berkeley National Laboratory, Modelica Buildings Library. https://simulationresearch.lbl.gov/modelica/userGuide/index.html. (Accessed February 8th, 2023).
[22] Energy Plus Weather Data. https://energyplus.net/weather. (Accessed February 8th, 2023).
[23] Executive Order on Building Regulation, (2018). https://bygningsreglementet.dk/.
[24] European Committee for Standardization. EN 16798-1:2019, Energy performance of buildings — Ventilation for buildings.
[25] K. Ahmed, A. Akhondzada, J. Kurnitski, B. Olesen, Occupancy schedules for energy simulation in new prEN16798-1 and ISO/FDIS 17772–1 standards, Sustain. Cities Soc. 35 (2017) 134–144, https://doi.org/10.1016/j.scs.2017.07.010.
[26] B. Gunay, W. Shen, B. Huchuk, C. Yang, S. Bucking, W. O'Brien, Energy and comfort performance benefits of early detection of building sensor and actuator faults, Build. Serv. Eng. Res. Technol. 39 (2018) 652–666, https://doi.org/10.1177/0143624418769264.
[27] R. Zhang, T. Hong, Modeling of HVAC operational faults in building performance simulation, Appl. Energy. 202 (2017) 178–188, https://doi.org/10.1016/j.apenergy.2017.05.153.
[28] J. Granderson, G. Lin, A. Harding, P. Im, Y. Chen, Building fault detection data to aid diagnostic algorithm creation and performance testing, Sci. Data 7 (2020) 1–14, https://doi.org/10.1038/s41597-020-0398-6.
[29] J. Verhelst, G. Van Ham, D. Saelens, L. Helsen, Economic impact of persistent sensor and actuator faults in concrete core activated office buildings, Energy Build. 142 (2017) 111–127, https://doi.org/10.1016/j.enbuild.2017.02.052.

[30] Y. Chen, S. Huang, D. Vrabie, A simulation based approach for impact assessment of physical faults: Large commercial building HVAC case study, ASHRAE IBPSA-USA Build, Simul. Conf. (2018) 823–830.
[31] S.H. Lee, F.W.H. Yik, A study on the energy penalty of various air-side system faults in buildings, Energy Build. 42 (2010) 2–10, https://doi.org/10.1016/j.enbuild.2009.07.004.
[32] L. Wang, T. Hong, Modeling and Simulation of HVAC Faulty Operation and Performance Degradation due to Maintenance Issues, ASim 2012 - 1st Asia Conf. Internatinal Build. Perform. Simul. Assoc. DE-AC02-05 (2014).
[33] Y. Li, Z. O'Neill, An innovative fault impact analysis framework for enhancing building operations, Energy Build. 199 (2019) 311–331, https://doi.org/10.1016/j.enbuild.2019.07.011.
[34] J. Kim, S. Frank, P. Im, J.E. Braun, D. Goldwasser, M. Leach, Representing small commercial building faults in energyplus, Part II: Model validation, Buildings 9 (2019), https://doi.org/10.3390/BUILDINGS9120239.
[35] J.Y. Kao, E.T. Pierce, Their Effects On Building Energy Consumpti on " The computer program BLAST-2 was used the performance of the air handling system " and cooling loads as well as simulate to calculate the building heating, (n.d.).
[36] S.T. Bushby, N. Castro, M.A. Park, G. Cheol, Using the Virtual Cybernetic Building Testbed and FDD Test Shell for FDD Tool Development NISTIR 6818 Using the Virtual Cybernetic Building Testbed and FDD Test Shell for FDD Tool Development, NIST Interagency/Internal Rep. NISTIR 6818 (2001).
[37] M. Padilla, D. Choinière, A combined passive-active sensor fault detection and isolation approach for air handling units, Energy Build. 99 (2015) 214–219, https://doi.org/10.1016/j.enbuild.2015.04.035.
[38] Y. Li, O. Zheng, An EnergyPlus/OpenStudio based Fault Simulator for Buildings, in: 2016 ASHRAE Winter Meet., 2016.
[39] Z. Shi, W. O'Brien, Using Building Performance Simulation for Fault Impact Evaluation, ESim 2018 (2018).
[40] ASHRAE Technical Committees, ASHRAE Fundamentals Handbook, (2001).
[41] The Modelica Association, Modelica. https://doc.modelica.org/om/Modelica.html. (Accessed February 8th, 2023).
[42] International Organization for Standardization, ISO 7730: Ergonomics of the thermal environment Analytical determination and interpretation of thermal comfort using calculation of the PMV and PPD indices and local thermal comfort criteria, 2005.